

Micrometer-Sized Water Droplets Induce Spontaneous Reduction

Jae Kyoo Lee,[†] Devleena Samanta,^{†,‡,Ⓛ} Hong Gil Nam,^{*,‡,§} and Richard N. Zare^{*,†,Ⓛ}

[†]Department of Chemistry, Stanford University, Stanford, California 94305, United States

[‡]Center for Plant Aging Research, Institute for Basic Science, Daegu 42988, Republic of Korea

[§]Department of New Biology, DGIST, Daegu 42988, Republic of Korea

Supporting Information

ABSTRACT: Bulk water serves as an inert solvent for many chemical and biological reactions. Here, we report a striking exception. We observe that in micrometer-sized water droplets (microdroplets), spontaneous reduction of several organic molecules occurs, pyruvate to lactate, lipoic acid to dihydrolipoic acid, fumarate to succinate, and oxaloacetate to malate. This reduction proceeds in microdroplets without any added electron donors or acceptors and without any applied voltage. In three of the four cases, the reduction efficiency is 90% or greater when the concentration of the dissolved organic species is less than 0.1 μM . None of these reactions occurs spontaneously in bulk water. One example demonstrating the possible broad application of reduction in water microdroplets to organic molecules is the reduction of acetophenone to form 1-phenylethanol. Taken together, these results show that microdroplets provide a new foundation for green chemistry by rendering water molecules to be highly electrochemically active without any added reducing agent or applied potential. In this manner, aqueous microdroplets might have provided a route for abiotic reduction reactions in the prebiotic era, thereby providing organic molecules with a reducing power before the advent of biotic reducing machineries.

Redox reactions, involving the transfer of electrons between a donor (reductant) and an acceptor (oxidant), are very common and are found in combustion, corrosion, and many other inorganic and organic chemical processes. Redox reactions also play a central role in living systems, including photosynthesis and respiration.¹ Water serves as an inert solvent for such organic, inorganic, and biological reactions. In stark contrast to the behavior in bulk water, here we report our finding that micrometer-sized water droplets (microdroplets) are able to induce reduction reactions of molecules without the addition of any other reducing agent, or externally applied charge.

Water microdroplets generated from bulk water exhibit distinct characteristics including reaction acceleration,^{2–9} altered thermodynamics,^{10,11} and molecular reorganization.¹² We have reported the spontaneous formation of gold nanostructures including nanoparticles and nanowires from precursor gold ions through the reduction of gold ions in microdroplets.¹³ Here, we investigate the reduction of organic

compounds in pure water microdroplets without using reducing agents, catalysts, or applying external charges.

Figure 1a presents a schematic of the experimental setup. Aqueous microdroplets (1 to 50 μm diameter in diameter)¹⁴ were generated by spraying bulk solution using dry N_2 nebulizing gas without applying an external voltage to the spray source. We sprayed solutions (10 μM) of four different molecules prepared in degassed water, pyruvate, lipoic acid, fumarate, and oxaloacetate. All these experiments were conducted at room temperature and atmospheric pressure.

Figure 1b–e presents the resulting mass spectra, showing spontaneous reduction of pyruvate (m/z 87.01, deprotonated) to lactate (m/z 89.02, deprotonated), lipoic acid (m/z 205.04, deprotonated) to dihydrolipoic acid (m/z 207.05, deprotonated), fumarate (m/z 115.00, deprotonated) to succinate (m/z 117.02, deprotonated), and oxaloacetate (m/z 131.00, deprotonated) to malate (m/z 133.01, deprotonated). Pyruvate, fumarate, and oxaloacetate were reduced by gaining two electrons and protons, and lipoic acid was reduced through cleavage of the disulfide bond. We essentially observed no molecular species other than reactants and reduced reactants in the mass range between 50 and 1000 m/z (Figure S1). It is important to note that these reductions do not occur in bulk water by themselves without adding appropriate reducing agents that can donate electrons.

Table 1 summarizes the reduced species observed in microdroplets along with their corresponding reduction efficiencies. The identities of the detected species were confirmed by tandem mass spectrometry using collision-induced dissociation (CID) (Figures S3–6). The reduction efficiency was calculated as detailed in the Supporting Information. Using mass spectrometry not employing microdroplets, we verified that the samples were initially free of impurities including reduced species. The lack of impurities and the conversion of pyruvate to lactate were also confirmed by ¹H nuclear magnetic resonance (NMR) (Figure S2).

We measured the kinetics of the reduction reaction for pyruvate to lactate by adjusting the traveling distance of microdroplets in air between the tip of the silica capillary and the mass spectrometer inlet (Figure 1a). Figure S7 shows the mass spectra of a 10 μM pyruvate solution in microdroplets at different traveling time points. We observed a gradual increase of lactate and decrease of pyruvate. The reaction time was estimated from the average speed of the microdroplet.² Figure

Received: March 25, 2019

Published: June 17, 2019



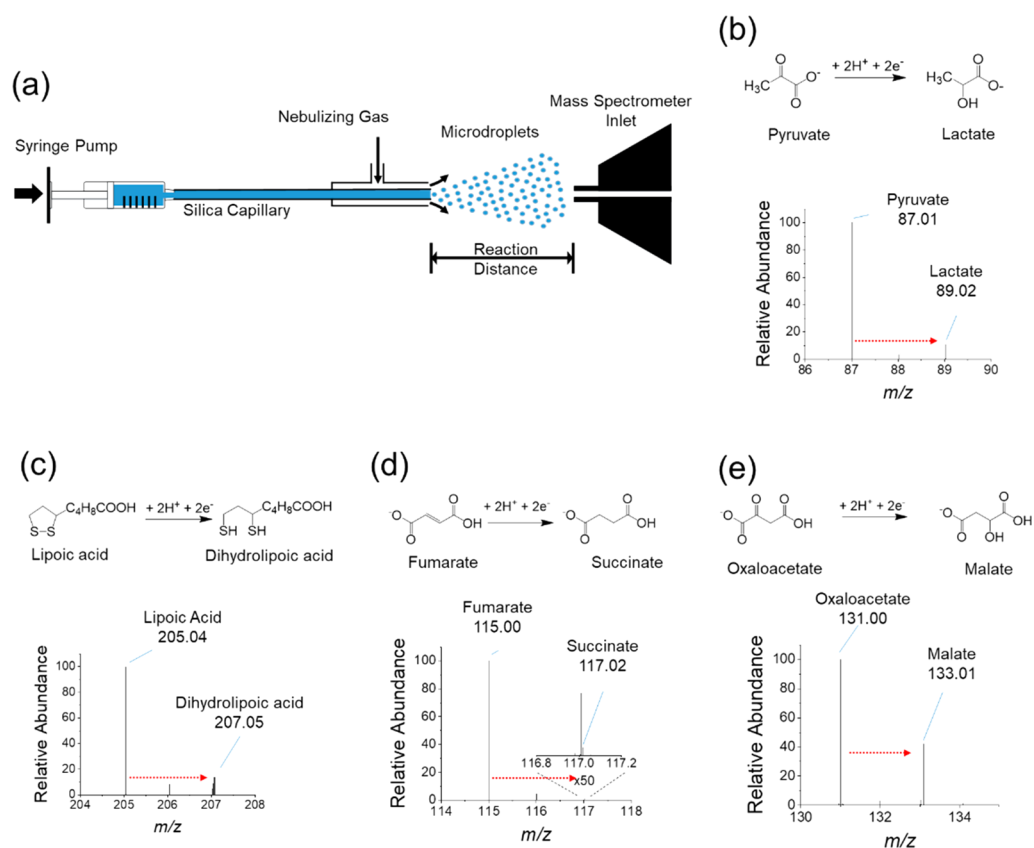


Figure 1. Mass spectrometric analysis of spontaneously reduced molecules in microdroplets. (a) Schematic of experiment setup for the redox reactions in microdroplets. (b–e). Mass spectra of pyruvate (b), lipoic acid (c), fumarate (d), and oxaloacetate (e) and their reduced species lactate, dihydrolipoic acid, succinate, and malate. The red arrows indicate the direction of the spontaneously reduced reactions in microdroplets.

Table 1. Summary of the Molecular Species That Have Undergone Spontaneous Reduction in Microdroplets

Original molecule	Observed molecule	Observed ion	Observed m/z	Theoretical m/z	Mass error (ppm)	Maximum reduction efficiency (%) ^a
Pyruvate	Lactate	M^-	89.02432	89.02387	5.08	91.6 ± 0.2 ^{b,c}
Lipoic acid	Dihydrolipoic acid	$[M - H]^-$	207.05170	207.05134	1.72	59.7 ± 13.6 ^d
Fumarate	Succinate	M^-	117.01940	117.01933	0.60	93.8 ± 5.0 ^e
Oxaloacetate	Malate	M^-	133.01295	133.01315	1.50	90.9 ± 11.2 ^f

^aThis reduction efficiency, calculated as detailed in the [Supporting Information](#), was measured at approximately 1.5 mm traveling distance. ^bThe error represents one standard deviation computed from four independent measurements. ^cVaries between 0.03 and 91.6%, depending on concentration. ^dVaries between 1.7 and 59.7%, depending on concentration. ^eVaries between 0.2 and 93.8%, depending on concentration. ^fVaries between 6.2 and 90.9%, depending on concentration.

2a presents how the reduction efficiency changes with microdroplet traveling time. We observed that the reduction reached a plateau ~3 ms after exposure of pyruvate molecules to the microdroplet environment. It should be noted that this time point is a rough estimate because the relationship between reaction distance and reaction time can be quantitatively determined up to 130 μ s of microdroplet traveling time.³ Beyond this limit, the effect of microdroplet evaporation becomes non-negligible, and therefore, the exact estimated time in which the reduction reaches a plateau cannot be precisely determined.³ Regardless, the fact that the extent of reduction varies with the travel time of the microdroplet before arriving at the mass spectrometer inlet supports the contention that reduction occurs while the molecules reside in the microdroplet. The kinetics of reduction is dependent on the concentration of reactant (Figure S8). A faster kinetics of reduction was observed for the reactant with a lower concentration.

The maximum reduction efficiency (Table 1) achieved was around 91% for pyruvate, fumarate, and oxaloacetate (Figures 2b, S9a, and S9c) and 60% for lipoic acid (Figure S9b) at the 1–10 nM concentration range. The reduction efficiency decreased as the reagent concentration increased, reaching an asymptotic value. We further observed a trend for increased reduction efficiency with decreasing microdroplet size (Figure 2c), i.e., with increased surface-to-volume ratio of microdroplets by increasing nebulizing gas pressure.¹⁵ We hypothesize that these observations on the reduction behavior can be explained by assuming that the reduction is confined primarily to the droplet surface.

We were able to confirm in a visual manner that the microdroplet causes reduction. We imaged aqueous microdroplets containing 100 nM resazurin, a water-soluble, reduction-sensitive dye.¹⁶ Resazurin emits fluorescence upon reduction (to resorufin) with a peak emission at 590 nm when excited by 570 light (Figure 3a). The resazurin solution was

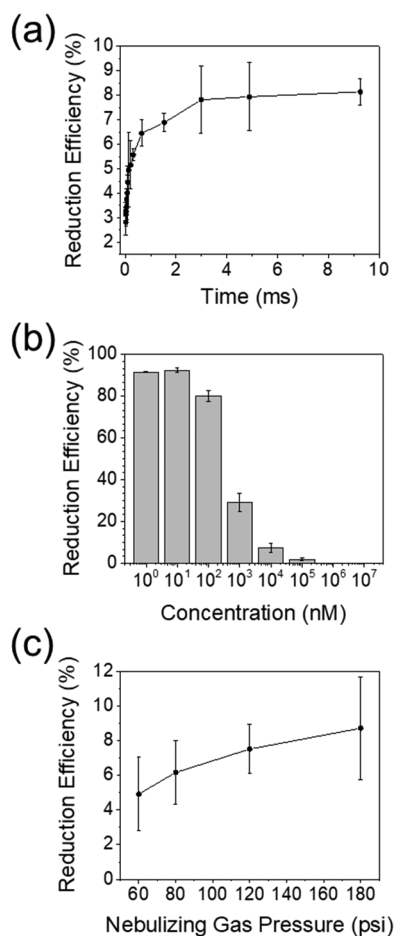


Figure 2. Characterization of spontaneous reduction of pyruvate to lactate in microdroplets: (a) kinetics of the reduction reaction of 10 μM pyruvate, (b) dependence of reduction efficiency on the concentration of pyruvate, and (c) effect of nebulization N_2 gas pressure on the reduction efficiency. The error bars represent one standard deviation from three independent measurements.

sprayed onto a glass coverslip and then each microdroplet was imaged with a confocal microscope (Figure 3b). Figure 3c shows the fluorescence image obtained with a 595–630 nm filter, and Figure 3d shows a brightfield image of the same microdroplet. It is evident that resazurin is reduced to resorufin as seen by the resorufin fluorescence. The reduction of resazurin to resorufin was also confirmed by mass spectrometrically analyzing microdroplets containing 1 μM resazurin (Figure S10).

Moreover, this reduction occurs without adding any reducing agent to the microdroplets and without applying any external voltage to the spray source. The localization of the resorufin at the periphery of the microdroplet is a consequence of its hydrophobicity as demonstrated by Figure S11. Thus, we are unable to locate with certainty where the reduction occurs. However, when this observation is combined with the variation of reduction with concentration as well as the increased reduction for smaller droplets that have higher surface-to-volume ratios, we argue that reduction is occurring at or near the microdroplet surface.

Taken together, these experiments conclusively demonstrate that the reduction proceeds spontaneously in microdroplets. However, the mechanism is not yet clear. The idea that heterogeneous environments between vapor and condensed

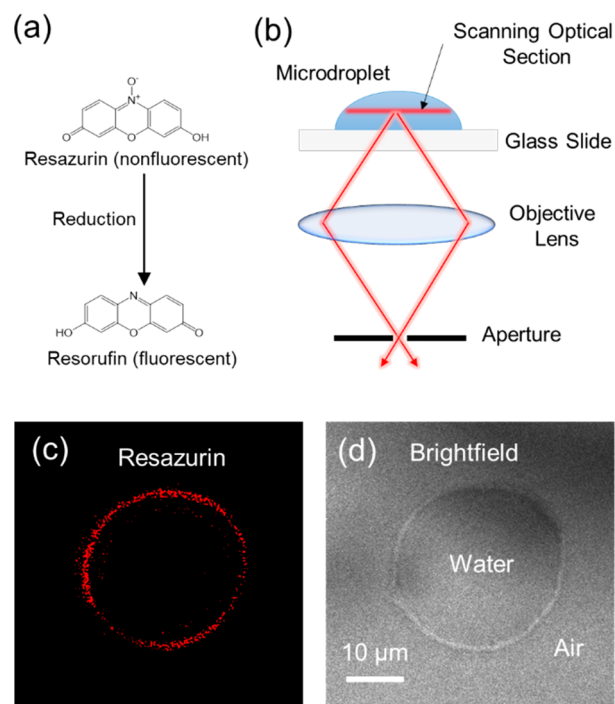


Figure 3. Confocal microscope images of a water microdroplet on a coverslip containing 100 nM reduction-sensitive dye, resazurin. (a) Reaction scheme of the reduction of resazurin. (b) Schematic of confocal imaging setup. (c) Fluorescent image of microdroplet. (d) Brightfield image of microdroplet.

phase or between different solvents could catalyze reactions is not new,^{17–19} but experimental investigations have been sparse. We suggest that OH^- at and near the microdroplet surface provides the likely source of electrons. (See Supporting Information for a more detailed discussion including possible effects of contact electrification,²⁰ triboelectrification,²¹ and charge separation during microdroplet fission.²²) As Ben Amotz²³ points out in a review of electron behavior in water, “it is becoming evident that electrons from one molecule or ion may often choose to distribute themselves promiscuously over neighboring molecules.” Although there are still debates concerning the value of the surface potential at the air–water interface,²⁴ a value for the strength of electric field at the air–water interface is estimated to be on the order of tens of million volts per centimeter.²⁵ A potential of approximately 3 V across the 5 \AA air–water interface²⁵ exceeds a standard potential of 1.23 V for the electrolysis of water molecules as well as a potential of 2.72 V for removing electrons from hydroxide ions to form hydroxyl radicals.²⁶ It needs to be stressed that this value refers to bulk water and not to the air–water interface, where OH^- might more readily give up its electron. Although there remains no consensus whether the surface of the microdroplet is acidic or basic,^{27–29} it appears that water autoionizes much more readily at the microdroplet surface forming both more OH^- and more H^+ than in bulk. We hypothesize that OH^- at the microdroplet periphery is oxidized to form hydroxyl radicals. We postulate we have some evidence that supports this hypothesis. We obtained that by capturing hydroxyl radicals with salicylic acid, which was converted into 2,5-dihydroxybenzoic acid.³⁰ Figure S12 shows mass spectra of microdroplets containing 10 μM salicylic acid without or with 10 nM pyruvate. In both cases, hydroxyl radicals captured by salicylic acid were observed. The

hypothesis that the large electric field at the water–air interface induces the reduction is further supported by the observation of the decrease in reduction efficiency by adding NaCl to microdroplets (Figure S13).

We understand that there could be another mechanism unforeseen at this stage. Vaida and co-workers have reported the pH dependence of the aqueous-phase photochemistry of α -keto acids.³¹ The pH of a water microdroplet differs from bulk although its value is still under debate.^{32,33} The pH at the water–air interface may even differ from the interior of microdroplets. The change in pH may be the influence of the redox potential of water, water ions, and compounds dissolved in microdroplets. Colussi and co-workers have reported distinct properties of chemical reactions occurring at the water-vapor phase, water-hydrophobic interface, and water–air interface.^{34–36} Francisco and co-workers reported that the pK_a and the redox potential at the water–air interface are different from the ones in bulk, suggesting the microdroplet surface provides an energetically favorable environment for redox reactions.^{19,37–39} Clearly, more work is needed to establish the mechanism concerning how pure water can cause reduction when put into the form of small droplets. Nevertheless, we postulate that the phenomenon of aqueous microdroplet reduction is clearly established by this study.

To illustrate the power of this method for reduction of organic compounds, we sprayed 10 μ M acetophenone (m/z 143.05, sodiated) in pure water and detected the reduced product, 1-phenylethanol (m/z 123.08, protonated) (Figure 4). See Figure S14 for the confirmation with CID. The production yield was approximately 28%.

We also suggest that microdroplet chemistry has another important implication. In many biological systems, energy is ultimately produced by converting light into chemical bonds through a series of reduction reactions of biomolecules

through complex photosynthesis machineries.⁴⁰ We have shown that microdroplets can abiotically induce reduction of biomolecules that are involved in the cellular energy cycle. This may provide a possible plausible route for the origin of nonenzymatic production of reduced biomolecules in a prebiotic era. Furthermore, as most biochemical reactions in living systems take place in cellular structures having the dimensions of microdroplets, our findings imply that cellular biochemistry inferred from bulk properties might need to be re-evaluated.

■ ASSOCIATED CONTENT

Supporting Information

The Supporting Information is available free of charge on the ACS Publications website at DOI: 10.1021/jacs.9b03227.

Experimental details (PDF)

■ AUTHOR INFORMATION

Corresponding Authors

*zare@stanford.edu

*nam@dgist.ac.kr

ORCID

Devleena Samanta: 0000-0002-0647-7673

Richard N. Zare: 0000-0001-5266-4253

Present Address

¹Department of Chemistry and International Institute for Nanotechnology, Northwestern University, 2145 Sheridan Road, Evanston, Illinois 60208, USA

Notes

The authors declare no competing financial interest.

■ ACKNOWLEDGMENTS

We dedicate this paper to the memory of Alexandra Hyunji Nam (1987–2017). D.S. expresses thanks for a Stanford Graduate Fellowship and for funding from the Center for Molecular Analysis and Design. We thank Shyam Sathyamoorthi for helpful discussions. This work was supported by the Air Force Office of Scientific Research through Basic Research Initiative grant (AFOSR FA9550-12-1-0400) and the Institute for Basic Science (IBS-R013-D1).

■ REFERENCES

- Halliwell, B. Reactive species and antioxidants. Redox biology is a fundamental theme of aerobic life. *Plant Physiol.* **2006**, *141* (2), 312–22.
- Lee, J. K.; Kim, S.; Nam, H. G.; Zare, R. N. Microdroplet fusion mass spectrometry for fast reaction kinetics. *Proc. Natl. Acad. Sci. U. S. A.* **2015**, *112* (13), 3898–3903.
- Lee, J. K.; Banerjee, S.; Nam, H. G.; Zare, R. N. Acceleration of reaction in charged microdroplets. *Q. Rev. Biophys.* **2015**, *48* (4), 437–444.
- Banerjee, S.; Zare, R. N. Syntheses of Isoquinoline and Substituted Quinolines in Charged Microdroplets. *Angew. Chem., Int. Ed.* **2015**, *54* (49), 14795–14799.
- Badu-Tawiah, A.; Campbell, D.; Cooks, R. G. Accelerated C-N Bond Formation in Dropcast Thin Films on Ambient Surfaces. *J. Am. Soc. Mass Spectrom.* **2012**, *23* (9), 1461–1468.
- Bain, R. M.; Pulliam, C. J.; Cooks, R. G. Accelerated Hantzsch electropray synthesis with temporal control of reaction intermediates. *Chem. Sci.* **2015**, *6* (1), 397–401.
- Fallah-Araghi, A.; Meguellati, K.; Baret, J.-C.; Harrak, A. E.; Mangeat, T.; Karplus, M.; Ladame, S.; Marques, C. M.; Griffiths, A. D. Enhanced Chemical Synthesis at Soft Interfaces: A Universal

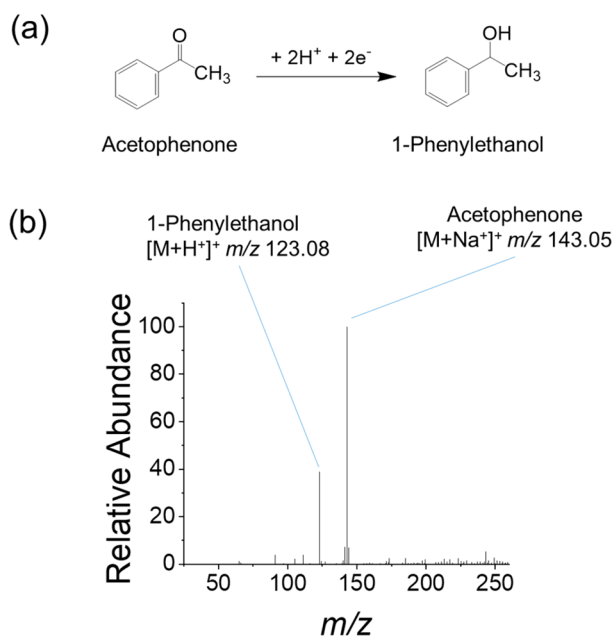


Figure 4. Green synthesis of 1-phenylethanol from acetophenone (10 μ M) using water microdroplets: (a) reaction scheme for the reduction of acetophenone to 1-phenylethanol and (b) mass spectrum of acetophenone and its reduced compound, 1-phenylethanol in microdroplets.

Reaction-Adsorption Mechanism in Microcompartments. *Phys. Rev. Lett.* **2014**, *112* (2), 028301.

(8) Girod, M.; Moyano, E.; Campbell, D. I.; Cooks, R. G. Accelerated bimolecular reactions in microdroplets studied by desorption electrospray ionization mass spectrometry. *Chem. Sci.* **2011**, *2* (3), 501.

(9) Müller, T.; Badu-Tawiah, A.; Cooks, R. G. Accelerated Carbon-Carbon Bond-Forming Reactions in Preparative Electrospray. *Angew. Chem., Int. Ed.* **2012**, *51* (47), 11832–11835.

(10) Nam, I.; Lee, J. K.; Nam, H. G.; Zare, R. N. Abiotic production of sugar phosphates and uridine ribonucleoside in aqueous microdroplets. *Proc. Natl. Acad. Sci. U. S. A.* **2017**, *114* (47), 12396–12400.

(11) Nam, I.; Nam, H. G.; Zare, R. N. Abiotic synthesis of purine and pyrimidine ribonucleosides in aqueous microdroplets. *Proc. Natl. Acad. Sci. U. S. A.* **2018**, *115* (1), 36–40.

(12) Zhou, Z.; Yan, X.; Lai, Y.-H.; Zare, R. N. Fluorescence Polarization Anisotropy in Microdroplets. *J. Phys. Chem. Lett.* **2018**, *9*, 2928–2932.

(13) Lee, J. K.; Samanta, D.; Nam, H. G.; Zare, R. N. Spontaneous formation of gold nanostructures in aqueous microdroplets. *Nat. Commun.* **2018**, *9* (1), 1562.

(14) Venter, A.; Sojka, P. E.; Cooks, R. G. Droplet dynamics and ionization mechanisms in desorption electrospray ionization mass spectrometry. *Anal. Chem.* **2006**, *78* (24), 8549–8555.

(15) Sulaiman, S. A.; Daud, M. H. Comparative Study of Droplet Sizes of Water and Diesel Sprays. *Asian J. Sci. Res.* **2013**, *6* (2), 367–373.

(16) Bueno, C.; Villegas, M.; Bertolotti, S.; Previtali, C.; Neumann, M.; Encinas, A. V. The excited-state interaction of resazurin and resorufin with amines in aqueous solutions. Photophysics and photochemical reaction. *Photochem. Photobiol.* **2002**, *76* (4), 385–390.

(17) Benjamin, I. Chemical reactions and solvation at liquid interfaces: A microscopic perspective. *Chem. Rev.* **1996**, *96* (4), 1449–1476.

(18) Bonn, M.; Nagata, Y.; Backus, E. H. Molecular Structure and Dynamics of Water at the Water–Air Interface Studied with Surface-Specific Vibrational Spectroscopy. *Angew. Chem., Int. Ed.* **2015**, *54* (19), 5560–5576.

(19) Zhong, J.; Kumar, M.; Francisco, J. S.; Zeng, X. C. Insight into chemistry on cloud/aerosol water surfaces. *Acc. Chem. Res.* **2018**, *51* (5), 1229–1237.

(20) Liu, C.; Bard, A. J. Electrostatic electrochemistry at insulators. *Nat. Mater.* **2008**, *7* (6), 505.

(21) Dumitrescu, I.; Anand, R. K.; Fosdick, S. E.; Crooks, R. M. Pressure-driven bipolar electrochemistry. *J. Am. Chem. Soc.* **2011**, *133* (13), 4687–4689.

(22) Tang, L.; Kebarle, P. Dependence of ion intensity in electrospray mass spectrometry on the concentration of the analytes in the electrosprayed solution. *Anal. Chem.* **1993**, *65* (24), 3654–3668.

(23) Ben-Amotz, D. Unveiling electron promiscuity. *J. Phys. Chem. Lett.* **2011**, *2* (10), 1216–1222.

(24) Paluch, M. Surface potential at the water-air interface. *Universitatis Mariae Curie-Sklodowska, sectio AA–Chemia* **2016**, *70* (2), 1.

(25) Kathmann, S. M.; Kuo, I. F. W.; Mundy, C. J. Electronic Effects on the Surface Potential at the Vapor–Liquid Interface of Water. *J. Am. Chem. Soc.* **2009**, *131* (47), 17522.

(26) Schwarz, H.; Dodson, R. Equilibrium between hydroxyl radicals and thallium (II) and the oxidation potential of hydroxyl (aq). *J. Phys. Chem.* **1984**, *88* (16), 3643–3647.

(27) Buch, V.; Milet, A.; Vácha, R.; Jungwirth, P.; Devlin, J. P. Water surface is acidic. *Proc. Natl. Acad. Sci. U. S. A.* **2007**, *104* (18), 7342–7347.

(28) Tse, Y.-L. S.; Chen, C.; Lindberg, G. E.; Kumar, R.; Voth, G. A. Propensity of hydrated excess protons and hydroxide anions for the air–water interface. *J. Am. Chem. Soc.* **2015**, *137* (39), 12610–12616.

(29) Agmon, N.; Bakker, H. J.; Campen, R. K.; Henschman, R. H.; Pohl, P.; Roke, S.; Thämer, M.; Hassanal, A. Protons and hydroxide ions in aqueous systems. *Chem. Rev.* **2016**, *116* (13), 7642–7672.

(30) Karnik, B. S.; Davies, S. H.; Baumann, M. J.; Masten, S. J. Use of salicylic acid as a model compound to investigate hydroxyl radical reaction in an ozonation–membrane filtration hybrid process. *Environ. Eng. Sci.* **2007**, *24* (6), 852–860.

(31) Rapp, R. J.; Dooley, M. R.; Kappes, K.; Perkins, R. J.; Vaida, V. pH dependence of the aqueous photochemistry of α -keto acids. *J. Phys. Chem. A* **2017**, *121* (44), 8368–8379.

(32) Wei, H.; Vejerano, E. P.; Leng, W.; Huang, Q.; Willner, M. R.; Marr, L. C.; Vikesland, P. J. Aerosol microdroplets exhibit a stable pH gradient. *Proc. Natl. Acad. Sci. U. S. A.* **2018**, *115* (28), 7272–7277.

(33) Craig, R. L.; Peterson, P. K.; Nandy, L.; Lei, Z.; Hossain, M. A.; Camarena, S.; Dodson, R. A.; Cook, R. D.; Dutcher, C. S.; Ault, A. P. Direct Determination of Aerosol pH: Size-Resolved Measurements of Submicrometer and Supramicrometer Aqueous Particles. *Anal. Chem.* **2018**, *90* (19), 11232–11239.

(34) Enami, S.; Mishra, H.; Hoffmann, M. R.; Colussi, A. J. Protonation and oligomerization of gaseous isoprene on mildly acidic surfaces: Implications for atmospheric chemistry. *J. Phys. Chem. A* **2012**, *116* (24), 6027–6032.

(35) Enami, S.; Stewart, L. A.; Hoffmann, M. R.; Colussi, A. J. Supercritical chemistry on mildly acidic water. *J. Phys. Chem. Lett.* **2010**, *1* (24), 3488–3493.

(36) Enami, S.; Hoffmann, M. R.; Colussi, A. J. Proton availability at the air/water interface. *J. Phys. Chem. Lett.* **2010**, *1* (10), 1599–1604.

(37) Kumar, M.; Zhong, J.; Zeng, X. C.; Francisco, J. S. Reaction of Criegee intermediate with nitric acid at the air–water interface. *J. Am. Chem. Soc.* **2018**, *140* (14), 4913–4921.

(38) Kumar, M.; Li, H.; Zhang, X.; Zeng, X. C.; Francisco, J. S. Nitric Acid–Amine Chemistry in the Gas Phase and at the Air–Water Interface. *J. Am. Chem. Soc.* **2018**, *140* (20), 6456–6466.

(39) Martins-Costa, M. T.; Anglada, J. M.; Francisco, J. S.; Ruiz-Lopez, M. F. Reactivity of atmospherically relevant small radicals at the air–water interface. *Angew. Chem., Int. Ed.* **2012**, *51* (22), 5413–5417.

(40) McConnell, I.; Li, G.; Brudvig, G. W. Energy conversion in natural and artificial photosynthesis. *Chem. Biol.* **2010**, *17* (5), 434–447.